Neurobiology of Disease 45 (2012) 851–861

Contents lists available at SciVerse ScienceDirect

Neurobiology of Disease

journal homepage: www.elsevier.com/locate/ynbdi

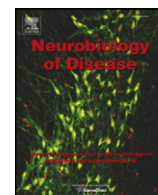

A new mouse model for the slow-channel congenital myasthenic syndrome induced by the AChR εL221F mutation

Frédéric Chevessier [a], Christoph Peter [a], Ulrike Mersdorf [a], Emmanuelle Girard [b], Eric Krejci [b], Joseph J. McArdle [c], Veit Witzemann [a,*]

[a] Department of Molecular Neurobiology, Max Planck Institute for Medical Research, Jahnstrasse 29, 69120 Heidelberg, Germany
[b] Université Paris Descartes, UMR 8194, Centre d'étude de la sensorimotricité, 75005 Paris, France
[c] New Jersey Medical School, University of Medicine and Dentistry of New Jersey, Newark, NJ 07103, USA

A R T I C L E I N F O

Article history:
Received 18 July 2011
Revised 29 September 2011
Accepted 28 October 2011
Available online 8 December 2011

Keywords:
Neuromuscular junction
Slow channel congenital myasthenic syndrome
Acetylcholine receptor
Mouse model
Homologous recombination

A B S T R A C T

We have generated a new mouse model for congenital myasthenic syndromes by inserting the missense mutation L221F into the ε subunit of the acetylcholine receptor by homologous recombination. This mutation has been identified in man to cause a mild form of slow-channel congenital myasthenic syndrome with variable penetrance. In our mouse model we observe as in human patients prolonged endplate currents. The summation of endplate potentials may account for a depolarization block at increasing stimulus frequencies, moderate reduced muscle strength and tetanic fade. Calcium and intracellular vesicle accumulation as well as junctional fold loss and organelle degeneration underlying a typical endplate myopathy, were identified. Moreover, a remodeling of neuromuscular junctions occurs in a muscle-dependent pattern expressing variable phenotypic effects. Altogether, this mouse model provides new insight into the pathophysiology of congenital myasthenia and serves as a new tool for deciphering signaling pathways induced by excitotoxicity at peripheral synapses.

© 2011 Elsevier Inc. All rights reserved.

Introduction

The slow-channel congenital myasthenic syndrome (SCCMS) is a rare neuromuscular junction disorder with an autosomal dominant pattern of inheritance characterized by progressive fatigable muscle weakness (Engel et al., 2003, 2010). SCCMS results from "gain-of-function" missense mutations in the muscle acetylcholine receptor (AChR) that enhance ACh affinity, gating efficiency, or both. The prolonged endplate currents of mutated AChRs cause excitotoxic injury by cationic overload at the postsynaptic region. So-called endplate myopathy is characterized by the destruction of junctional folds, loss of AChRs, focal degeneration of postsynaptic organelles, and apoptosis of the junctional nuclei (Engel et al., 2003; Milone et al., 1997; Vohra et al., 2004, 2006). Calcium accumulation identified in the subsynaptic compartment is likely to originate from the increased influx of calcium through the postsynaptic membrane during muscle stimulation accompanied by enhanced calcium release from the sarcoplasmic reticulum mainly via inositol-1, 4, 5-triphosphate receptors (IP3R) (Zayas et al., 2007).

The twenty slow-channel mutations described so far for man are distributed in different functional domains of the four AChR subunits (Engel et al., 2010; Outteryck et al., 2009). The majority of these mutations are located in the second transmembrane domain (M2) lining the pore of the AChR and prolong the mean channel open time. Only a few mutations were described in the first transmembrane domain (M1). The L221F mutation was identified in two unrelated families presenting mild myasthenic syndromes in the heterozygous patients (Chauplannaz and Bady, 1994; Croxen et al., 2002; Oosterhuis et al., 1987). Located near the extracellular end of transmembrane segment M1, the mutation is away from the acetylcholine binding site, as well as from the ion channel domain formed by the M2 segments. *In vitro* expression studies suggest that this mutation acts mainly by enhancing the affinity for acetylcholine, which causes repeated channel reopenings during the prolonged receptor occupancy slowing the decay of miniature synaptic currents. A smaller increase in channel opening rate and mean open time may also contribute to the slowed decay of miniature synaptic currents (Hatton et al., 2003). In addition, during the prolonged deactivation phase an increased fraction of AChR may become desensitized (Elenes et al., 2009) thus impairing neuromuscular transmission.

In patients, the expression of characteristic SCCMS phenotypes was variable. Some patients were asymptomatic but showed typical electrophysiological features found in SCCMS (i.e. repetitive compound muscle action potentials elicited by single stimuli). In more affected patients, the clinical symptoms, starting at early adult stage, were characterized by weakness of finger extensor muscles, wrist, neck muscles and by a slight weakness of other muscle groups

* Corresponding author at: Jahnstrasse 29, 69120 Heidelberg, Germany. Fax: +49 6221 486498.
E-mail address: witzeman@mpimf-heidelberg.mpg.de (V. Witzemann).
Available online on ScienceDirect (www.sciencedirect.com).

0969-9961/$ – see front matter © 2011 Elsevier Inc. All rights reserved.
doi:10.1016/j.nbd.2011.10.024

(Croxen et al., 2002; Oosterhuis et al., 1987). The endplate myopathy was relatively moderate compared to other genetically characterized SCCMS (Engel et al., 2003; Ohno et al., 1995). Calcium accumulations were only observed at an ultrastructural level and only few myopathic changes were identified in muscle biopsies (Oosterhuis et al., 1987).

The εL221F mutation leads to repeated channel reopenings and not to longer channel open times as in the majority of SCCMS, probably causing a different cation overload. It is, however, not known whether this difference accounts for different phenotypic expressivity and thus different disease symptoms in this form of SCCMS. Therefore we targeted the mouse AChR ε subunit gene by homologous recombination to obtain homozygous $AChR^{\varepsilon L221F/\varepsilon L221F}$ mice and analyzed different parameters at individual NMJs as well as in the entire muscle to demonstrate the pathological effect of this mutation. This mouse model represents a new tool to analyze variable phenotypic effects in muscle as well as to elucidate mechanisms involved in SCCMS genesis, the role of calcium and the consequences of excitotoxicity on NMJ maintenance.

Materials and methods

All experiments on mice were performed in accordance with European Community guidelines for laboratory animal handling. Use and care of animals followed German national laws and was approved by German authorities (TierSchG 117; IBF Universität Heidelberg MPI/T-13/08).

Mutagenesis

The L221F mutation was inserted into the cDNA of the mouse AChR ε subunit using the Quikchange® Site-directed mutagenesis kit according to the manufacturer's guidelines (Stratagene). The following oligonucleotides were used: 5′ CCG CCG GAA GCC GTT TTT TTA CGT CAT TAA C 3′ and 5′ GTT AAT GAC GTA AAA AAA CGG CTT CCG GCG G 3′. The sequence was then verified by a complete sequencing of mutated cDNA using the 3730 DNA-Analyzer (Applied Biosystems, Darmstadt, Germany).

Gene targeting

The *Not*I-linearized targeting vector containing a neomycin resistance cassette was introduced into E14-1 embryonic stem cells by electroporation (Kuhn et al., 1991). After 2 weeks of G418 selection, resistant colonies were isolated and cultivated further on. A first screen was performed by PCR after genomic DNA isolation of each colony using DNeasy 96 tissue kit (Qiagen, Hilden, Germany). The oligonucleotides used in the PCR reaction were the following 5′ CCA CAT ACA CTT CAT TCT CAG 3′ and CAG AAT GCC CAC AGA CGA G′ and generated a 1.5 kb fragment. The PCR fragments were blotted to a Hybound N^+ Membrane (GE Healthcare Europe GmbH, Freiburg, Germany) and hybridized with a fluorescein-labeled probe (5′ CCT CTC CCC CTT TTA TTC CCA TCC CTC AGC CTC CCA GAG CAG CAC CTC TA 3′). The probe was recognized by an HRP anti-fluorescein antibody and detected using the ECL-detection system (Roche Diagnostics Deutschland GmbH, Mannheim, Germany). A large scale genomic preparation of selected clones bearing the construct by homologous recombination was performed using the Blood and Cell Culture DNA Maxi Kit (Qiagen, Hilden, Germany), digested with *Hind*III and analyzed by Southern blotting. After sequencing, selected ES-cells were injected into C57Bl/6 blastocysts (F. Zimmerman, IBF, Heidelberg). Germline transmission was achieved and breeding of heterozygous mice resulted in homozygous $AChR^{\varepsilon L221F/\varepsilon L221F}$ mice.

Primers for identifying the WT epsilon allele were: forward 5′ GCTGGGCAGGTAATCTCAAAGTGG3′ and reverse 5′ GACCCCCTGGAATCCGACAAGT 3′.

PCR parameters were: 1 cycle 95 °C for 15 min; 34 cycles of 95 °C for 45 s, 64 °C for 45 s, 72 °C for 2 min; followed by 1 cycle of 72 °C for 10 min.

Primers for identifying the εL221F allele were: forward 5′ GGCCAGCTCATTCCTCCC ACTCAT 3′ and reverse 5′ GCTCCGCCTCAACCTCCCAACC 3′. PCR parameters were the same as described above but the annealing temperature was 61 °C.

The PCR products were separated on agarose gels and visualized with Ethidium Bromide.

RNA isolation and real-time PCR

RNA and real-time PCR were performed as described previously (Chevessier et al., 2008).

Relative quantification of PCR product synthesis was performed using “Assay on Demand” primers according to the recommendations of the manufacturer Applied Biosystems. The expression levels were normalized to the transcription level of the housekeeping enzyme glyceraldehyde 3 phosphate dehydrogenase GAPDH. The following primers were used: AChR ε subunit, Mm00437406_g1 (exon boundary 3–4) and GAPDH, Mm99999915_g1.

Ex vivo electrophysiological studies

Following exposure to carbon dioxide, mice were euthanized with cervical dislocation. Nerve–muscle preparations were prepared. The muscles studied were the hindlimb *Extensor digitorum longus* (EDL) and *Soleus* (SOL) as well as the thoracic *Triangularis sterni* (TS) muscle. Nerve–muscle preparations were pinned to a Sylgard-lined Plexiglass chamber containing (mM): NaCl (135), KCl (5.4), $MgCl_2$ (1), $CaCl_2$ (2), D-glucose (5.5), and HEPES (5.0; pH 7.2; 22 °C). Nerve was drawn into glass suction electrodes and stimulated with supra maximal square pulses (1 ms) to elicit endplate potentials (EPPs). To prevent muscle mechanical activity in response to nerve stimulation (1, 20, 50, or 70 Hz) 1 μM μ-Conotoxin GIIIB (Alomone Labs, Jerusalem, Israel) was added to the physiological solution. Spontaneous (MEPPs) and stimulus-evoked EPPs were recorded with sharp electrodes filled with 3 M KCl (10 to 20 MΩ). As an indicator of EPP summation, the % of change from the basal membrane potential is calculated for the first 4 to 6 EPPs during trains of stimuli at 50 and 70 Hz. That is, the difference in resting potential before and during the first 4–5 EPPs at stimulus frequencies of 50 and 70 Hz was expressed as a percentage of the pre-stimulus resting potential. Miniature endplate currents (MEPCs) were recorded with extracellular electrodes (1 MΩ) containing the physiologic solution. Endplate electrical signals recorded with an Axoclamp-2A amplifier (Axon Instruments, Union City, CA, USA) were digitized (Digidata 1321A, Axon Instruments) at 10,000 samples/s. PCLAMP software (Axon Instruments, version 9.2) saved the digitized data to disk for subsequent off-line analyses.

We have analyzed the MEPC data according to the following protocol. Baseline for continuous MEPC records was set to 0 mV and Clampfit software automatically created event files of single MEPCs. Each MEPC in an event file was fit with a first order exponential function to measure the time constant of decay (τ). Those τ values obtained from MEPCs whose amplitude was less than two times the mean + standard deviation of the baseline noise or from MEPCS whose decay phase was contaminated by another MEPC event were excluded. Thus, individual τ values were used to prepare the histograms of Fig. 2.

Grip strength measurement

Grip strength measurement was performed as described (Chevessier et al., 2008). To summarize, mice (3 months old) were allowed to grasp the triangular ring of a computerized electronic

Download English Version:

https://daneshyari.com/en/article/6022657

Download Persian Version:

https://daneshyari.com/article/6022657

Daneshyari.com